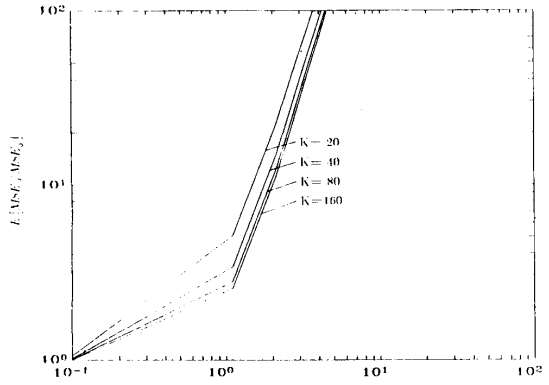

Fig. 5. Average MSE/MSE_o of the SMI method in the Griffiths array versus optimum SNR with the desired signal absent and $N = 4$.

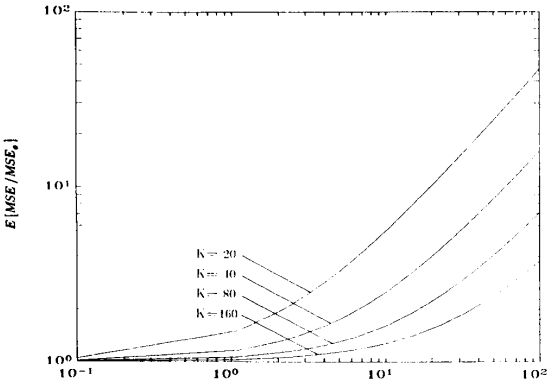

Fig. 6. Average MSE/MSE_o of the SMI method in the Griffiths array versus optimum SNR with the desired signal present and $N = 4$.

method when used in the constrained LMS array. In Figs. 1 and 3, as the input SNR increases, the optimum SNR also increases, and the MSE and the TOP performance is tremendously improved in the constrained LMS array with the desired signal absent. Figs. 5 and 6 show that for the Griffiths array, the MSE performance is better with the desired signal present than with the desired signal absent. This is due to the fact that the optimum weight vector is dependent on the received signal covariance matrix which would only be the noise covariance matrix if the desired signal is not present. When the optimum SNR increases, the average MSE in the Griffiths array becomes very large.

Moreover, we observe that if the optimum SNR is greater than three, the application of the SMI method in the constrained LMS array gives superior results, in the MSE sense, than in the Griffiths array. As the optimum SNR becomes small enough, this superiority is lost.

V. Conclusion

In this communication, we have derived the adaptive weight vector and the performance for the applications of the SMI method in the constrained LMS array and the Griffiths array. This work provides the performance characteristics of the SMI method for the selected array configurations and signal conditions. We have shown that in the constrained LMS array, the presence of the desired signal degrades the MSE and the TOP performance, while in the Griffiths array, the presence of the desired signal does not lower the MSE performance. Application of the SMI method in the constrained LMS array gives better performance, in the MSE sense, than in the Griffiths array when the optimum SNR is higher than a threshold; but worse when the optimum SNR is small enough.

References

[1] B. Widrow, P. E. Mantery, L. J. Griffiths, and B. B. Goode, "Adaptive antenna systems," *Proc. IEEE*, vol. 55, pp. 2143-2159, Dec. 1967.

[2] S. P. Applebaum, "Adaptive arrays," *IEEE Trans. Antennas Propagat.*, vol. AP-24, pp. 585-598, Sept. 1976.

[3] I. S. Reed, J. D. Mallett, and L. E. Brennan, "Rapid convergence rate in adaptive arrays," *IEEE Trans. Aerospace Electron. Syst.*, vol. AES-10, pp. 853-863, Nov. 1974.

[4] T. W. Miller, "The transient response of adaptive arrays in TPMA systems," Ph.D. dissertation, Dept. Elec. Eng., Ohio State Univ., Columbus, OH, 1976.

[5] L. L. Horowitz, "Convergence rate of the extended SMI algorithm for narrowband adaptive arrays," *IEEE Trans. Aerospace Electron. Syst.*, vol. AES-16, pp. 738-740, Sept. 1980.

[6] O. L. Frost, III, "An algorithm for linearly constrained adaptive array processing," *Proc. IEEE*, vol. 60, pp. 926-935, Aug. 1972.

[7] L. J. Griffiths, "A simple adaptive algorithm for real-time processing in antenna arrays," *Proc. IEEE*, vol. 57, pp. 1696-1704, Oct. 1969.

[8] J. Capon and N. R. Goodman, "Probability distributions for estimators of the frequency-wavenumber spectrum," *Proc. IEEE*, vol. 58, pp. 1785-1786, Oct. 1970.

A New Model for Calculating the Input Impedance of Coax-Fed Circular Microstrip Antennas with and Without Air Gaps

F. ABBOUD, J. P. DAMIANO, AND A. PAPIERNIK

Abstract—**A new model is presented for calculating the input impedance of a probe-fed circular antenna with and without air gaps between the substrate and the ground plane. It is based on the cavity model, the dynamic permittivity constant (to take into account the influence of the fringing field at the edge of radiating element), and the resonant parallel R–L–C circuit with an inductive reactance. Numerical results are compared with experimental ones. This model is well suited for computer-aided design.**

I. Introduction

A number of methods have been developed for the determination of the input impedance and the radiation pattern of circular microstrip antenna with probe excitation fed from a coaxiall line [1]-[5]. The numerical methods are time-consuming, while the analytical methods, though less accurate, enable the computation to be done with ease. For engineering applications, less accurate results are often sufficient. These results can be obtained rapidly with simple methods

Manuscript received November 18, 1988; revised August 10, 1989.

The authors are with the Laboratoire d'Electronique GDR CNRS Microantennes, Université de Nice-Sophia Antipolis, Parc Valrose, 06034 Nice cedex, France.

IEEE Log Number 9036302.

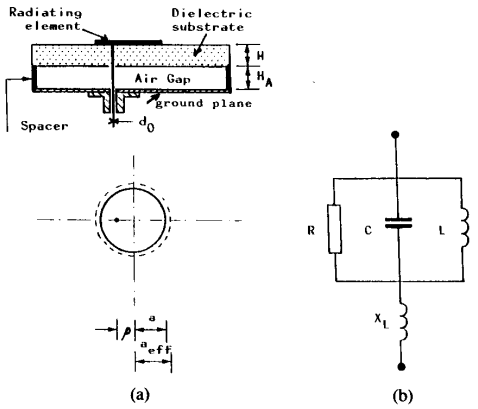

Fig. 1. (a) Geometry of a circular-disk microstrip antenna with an air gap. (b) Equivalent resonant parallel *R-L-C* circuit.

such as the cavity model [2]–[6], which suitably describe resonant frequency, input inpedance, bandwidth and the radiation pattern by a simple design equation.

Fig. 1(a) presents a circular microstrip antenna with an air gap between the substrate and the ground plane. this structure has been proposed by Dahele [7], [8] and Lee [9]. A decrease in the dynamic permittivity (increase of the air gap), results in an upward shift in the resonant frequency. Currently, most of the design formulas for the input impedance are only accurate for substrates of the order of $H/\lambda < 0.02$, where H is the thickness of the dielectric substrate and λ is the wavelength in the dielectric. Here, an analytic formula is derived for the input impedance of a circular microstrip antenna using the cavity model and the equivalent resonant circuits.

II. Equivalent Permittivity

The circular microstrip antenna is modeled as a cavity with a magnetic wall along the edge. This is in fact a two-layer cavity: the upper layer is the dielectric substrate of thickness H with relative permittivity ϵ_r and the lower layer is an air gap of thickness H_A with relative permittivity equal to one.

We use an equivalent single-layer structure of total height $H_T = H + H_A$ and an equivalent permittivity ϵ_{re} [9]:

$$\epsilon_{re} = \frac{\epsilon_r(H + H_A)}{(H + H_A\epsilon_r)}. \tag{1}$$

III. Calculation of the Resonant Frequency

An analytical formula is derived for the resonant frequency [10] of the transverse magnetic (TM) modes in a circular microstrip patch antenna given by

$$f_{nm} = \frac{\alpha_{nm} \cdot C}{2 \cdot \pi \cdot a_{\text{eff}} \cdot \sqrt{\epsilon_{\text{dyn}}}} \tag{2}$$

where c is the velocity of light in free space and α_{nm} is the mth zero of the derivative of the Bessel function of order n. The dominant mode is the TM_{11} mode ($n = m = 1$). For this mode, $\alpha_{11} = 1.84118$. ϵ_{dyn} is the dynamic permittivity introduced by Wolff [11]. It depends on the dimensions (a, $2H_T$), the equivalent permittivity ϵ_{re}, and the field distribution of the mode under study. It is given by

$$\epsilon_{\text{dyn}} = C_{\text{dyn}}(\epsilon)/C_{\text{dyn}}(\epsilon_0) \tag{3}$$

where $C_{\text{dyn}}(\epsilon)$ is the total dynamic capacitance of the condenser formed by the conducting patch and the ground plane separated by a dielectric of permittivity ϵ. It takes into account the influence of the fringing field at the edge of the circular microstrip antenna. $C_{\text{dyn}}(\epsilon_0)$ is the total dynamic capacitance when $\epsilon = \epsilon_0$.

$C_{\text{dyn}}(\epsilon)$ can be written [11, eq. 16] as

$$C_{\text{dyn}}(\epsilon) = C_{o,\text{dyn}}(\epsilon) + C_{e,\text{dyn}}(\epsilon). \tag{4}$$

$C_{o,\text{dyn}}(\epsilon)$ is the dynamic main capacitance of the dominant mode TM_{11} related to the static main capacitance $C_{o,\text{stat}}(\epsilon)$ of the patch without considering the fringing field. It is given by [11, eq. 14]:

$$C_{o,\text{dyn}}(\epsilon) = 0.3525 \cdot C_{o,\text{stat}}(\epsilon) \tag{5}$$

$$C_{o,\text{stat}}(\epsilon) = \epsilon_0 \cdot \epsilon_{re} \cdot \pi \cdot a^2/H_T. \tag{6}$$

$C_{e,\text{dyn}}(\epsilon)$ represents the dynamic fringing capacitance of the dominant mode given by [11, eq. 15]:

$$C_{e,\text{dyn}}(\epsilon) = \frac{1}{2}C_{e,\text{stat}}(\epsilon) \tag{7}$$

where $C_{e,\text{stat}}(\epsilon)$ represents the static fringing capacitance of the dominant mode due to the fringing field at the edge. It was studied by Chew [12]. We replace the static fringing of Wolff [11] by the one given by Chew [12, eq. 33]:

$$C_{e,\text{stat}}(\epsilon) = \frac{\epsilon_0 \cdot \epsilon_{re} \cdot \pi \cdot a^2}{H_T}\left\{1 + \frac{2 \cdot H_T}{\pi \cdot \epsilon_{re} \cdot a}\left[\log\left(\frac{a}{2 \cdot H_T}\right) + (1.41\epsilon_{re} + 1.77) + \frac{H_T}{a}(0.268\epsilon_{re} + 1.65)\right]\right\}. \tag{8}$$

Chew [12] shows this expression to be better than Shen's formula [13].

$C_{\text{dyn}}(\epsilon_0)$ can be obtained similarly as $C_{\text{dyn}}(\epsilon)$ by replacing ϵ by ϵ_0 in all of the above formulas.

From (8), it is possible to define a novel effective radius a_{eff} which is valid for $H_T/a < 0.5$ and $\epsilon_{re} < 10$:

$$a_{\text{eff}} = a\left\{1 + \frac{2 \cdot H_T}{\pi \cdot \epsilon_{re} \cdot a}\left[\log\left(\frac{a}{2 \cdot H_T}\right) + (1.41\epsilon_{re} + 1.77) + \frac{H_T}{a}(0.268\epsilon_{re} + 1.65)\right]\right\}^{1/2}. \tag{9}$$

IV. Calculation of the Input Impedance

The circular microstrip antenna can be considered as a resonant cavity modeled by a single resonant parallel *R-L-C* (Fig. 1(b)). All expressions presented hereafter are valid for the dominant mode. The resonant frequency is f_R. the input impedance is given by

$$Z(f) = \frac{R(\rho)}{1 + Q_T^2\left[\frac{f}{f_R} - \frac{f_R}{f}\right]^2} + j\left\{X_L - \frac{R(\rho) \cdot Q_T \cdot \left[\frac{f}{f_R} - \frac{f_R}{f}\right]}{1 + Q_T^2\left[\frac{f}{f_R} - \frac{f_R}{f}\right]^2}\right\} \tag{10}$$

where Q_T is the quality factor associated with system losses and $R(\rho)$ is the input resistance at the resonance (the resistance R of the *R-L-C* circuit). Q_T includes radiation losses Q_R, dielectric losses Q_D and conductor losses Q_C.

$$Q_T = \left[\frac{1}{Q_R} + \frac{1}{Q_C} + \frac{1}{Q_D}\right]^{-1}. \tag{11}$$

1) Q_R has the following form after some transformations from the expressions given by Bahl [5, eq. 3.27, eq. 3.44]:

$$Q_R = \frac{4 \cdot a \cdot (\alpha_{11}^2 - 1) \cdot \epsilon_{re}^{3/2}}{H_T \cdot \alpha_{11}^3 \cdot F(\alpha_{11}/\sqrt{\epsilon_{re}})} \tag{12}$$

where $F(X)$ is given by the following expression with the help of the development of Bessel function J_0 [14]:

$$F(X) = \frac{4}{X^3}\left\{2 \cdot X \cdot J_0(2X) + (X^2 - 1)\int_0^{2X} J_0(t) \cdot dt\right\} \tag{13}$$

$$F(X) = 2.666667378 - 1.066662519X^2 + 0.209534311X^4 - 0.019411347X^6 + 0.001044121X^8 - 0.000049747X^{10}. \tag{14}$$

2) The dielectric losses have been obtained by [1]

$$Q_D = 1/(\tan\delta)_{re} \tag{15}$$

where $(\tan\delta)_{re}$ is the equivalent dielectric loss tangent calculated with (1) where ϵ_r is taken as complex.

3) The losses in the conductor can be obtained by [1], [15]:

$$Q_C = H_T/\delta_s,\ \delta_s = (\pi \cdot f \cdot \mu_0 \cdot \sigma)^{-1/2}. \tag{16}$$

δ_s is the skin depth where σ is the conductivity of the conductor and μo is the permeability of the dielectric. $R(\rho)$ is the resonant resistance of the resonant parallel R-L-C circuit [16, eq. 10] which is given by

$$R(\rho) = \frac{1}{G_T}\frac{J_1^2(K \cdot \rho)}{J_1^2(K \cdot a)} \tag{17}$$

where ρ is the feed position referred to the center of the disk of radius a. K is the propagation constant. The fundamental mode corresponds to Ka equal to α_{11} as 1.84118 and G_T includes the conductances due to ohmic, dielectric and radiation losses:

$$G_T = G_R + G_D + G_C. \tag{18}$$

1) The conductance due to radiation losses is given by [15]

$$G_R = \frac{2.39}{4 \cdot \mu_0 \cdot H_T \cdot f_R \cdot Q_R}. \tag{19}$$

2) The conductance due to dielectric losses is given by [16, eq. 8]:

$$G_D = \frac{2.39 \cdot \tan\delta}{4 \cdot \mu_0 \cdot f_R \cdot H_T}. \tag{20}$$

3) The conductance due to ohmic losses is given by [16, eq. 9]:

$$G_C = \frac{2.39 \cdot \pi \cdot (\pi \cdot f_R \cdot \mu_0)^{-3/2}}{4 \cdot H_T^2 \cdot \sqrt{\sigma}}. \tag{21}$$

The Bessel function of order one, J_1, is expanded in terms of polynomial [14], for $-3 < t < 3$:

$$J_1(t) = t(0.5 - 0.56249985(t/3)^2 + 0.21093573(t/3)^4 - 0.03954289(t/3)^6 + 0.00443319(t/3)^8 - 0.0031761(t/3)^{10}). \tag{22}$$

It may be necessary to take into account the coax-fed probe by an inductive term of which the expression is given by Deshpande [17]:

$$X_L = \frac{377 \cdot f \cdot H}{c}\log\left(\frac{c}{\pi \cdot f \cdot d_0\sqrt{\epsilon_{re}}}\right). \tag{23}$$

TABLE I
COMPUTED AND MEASURED VALUES OF RESONANT FREQUENCY (IN GHz) WITHOUT AN AIR GAP, FOR THE FUNDAMENTAL MODE TM_{11}

a(mm)	H/λ	Itoh	Howell	Wolff	Derneryd	our
		Measure				Model
		[18]	[19]	[11]	[16]	
11.5	0.038	4.425	4.695	4.538	4.341	4.413
10.7	0.041	4.723	5.046	4.866	4.646	4.723
9.6	0.045	5.224	5.625	5.404	5.143	5.226
8.2	0.052	6.074	6.585	6.289	5.956	6.047
7.4	0.057	6.634	7.297	6.939	6.549	6.644

ϵ_r = 2.65, H = 1.5875 mm

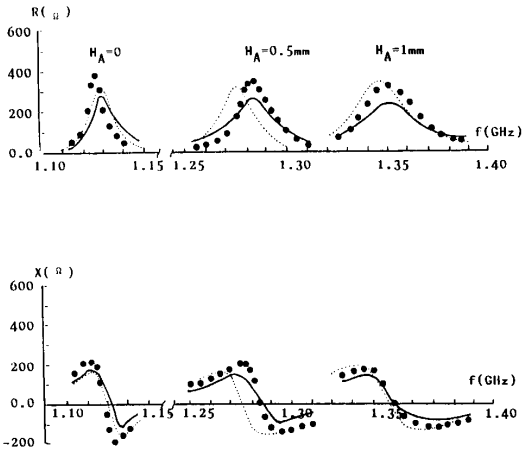

Fig. 2. Input impedance of coax-fed microstrip patch antenna of TM_{11} for three values of the air gap width H: $\epsilon_r = 2.32$, $\tan\delta = 0.001$, $H = 1.59$ mm, $d_0 = 1.27$ mm, $Z_0 = 50\Omega$, $a = 50.00$ mm, $\rho = 47.50$ mm; ..... measured [9], ... calculated [9], __ our model.

V. Results

In this section, numerical results using the above described model for the fundmaental mode are compared with measurements and previous computations.

A. Case of the Resonant Frequency

The lowest resonant frequency is calculated and compared with that obtained from the models of Howell [19], Wolff [11], and Derneryd [16] in Table I. We observe that our results fall among those calculated by the other three methods, and are closer to measured values (Itoh [18]) in all cases.

B. Case of the Input Impedance

Fig. 2 shows the input impedances of the TM_{11} mode for three air gap values H_A. Our computations are compared with the computed results and measurements of Lee [9]. Our theoretical values are in good enough agreement with the experimental one.

VI. Conclusion

In this paper, we have presented a simple model yielding the input impedance of a probe-fed circular microstrip antenna with and without air gaps. This simple model can be used successfully in computer-aided design of microstrip antenna arrays.

References

[1] S. A. Long, L. C. Shen, and P. B. Morel, "Theory of the circular-disc printed-circuit antenna," *Inst. Elec. Eng. Proc.*, vol. 125, pt. H, no. 10, pp. 925-928, 1978.

[2] M. Davidovitz and Y. T. Lo, "Input impedance of a probe-fed circular microstrip antenna with thick substrate," *IEEE Trans. Antennas Propagat.*, vol. AP-34, pp. 905–911, July 1986.
[3] Y. T. Lo, D. Solomon, and W. F. Richards, "Theory and experiment on microstrip antennas," *IEEE Trans. Antennas Propagat.*, vol. AP-27, pp. 137–145, Mar. 1979.
[4] S. Yano and A. Ishimaru, "A theoretical study of the input impedance of a circular microstrip disk antenna," *IEEE Trans. Antennas Propagat.*, vol. AP-29, pp. 77–83, Jan. 1981.
[5] I. J. Bahl and P. Bhartia, *Microstrip Antennas*. Dedham, MA: Artech House, 1980.
[6] F. Abboud, J. P. Damiano, and A. Papiernik, "Simple model for the input impedance of coax-fed rectangular microstrip patch antenna for C.A.D.," *Inst. Elec. Eng. Proc.*, vol. 135, pt. H, no. 5, pp. 323–326, 1988.
[7] J. S. Dahele and K. F. Lee, "Theory and experiment on microstrip antennas with airgaps," *Inst. Elec. Eng. Proc.*, vol. 132, pt. H, no. 7, pp. 455–460, 1985.
[8] ——, "A dual-frequency circular disk microstrip antenna with tunable characteristics," in *Proc. 12th European Microwave Conf.*, Helsinki, 1982, pp. 390–395.
[9] K. F. Lee, K. Y. Ho, and J. S. Dahele, "Circular-disk microstrip antenna with an air gap," *IEEE Trans. Antennas Propagat.*, vol. AP-32, pp. 880–884, Aug. 1984.
[10] F. Abboud, J. P. Damiano, and A. Papiernik, "A new determination of the resonant frequency of a circular disc microstrip antenna: Application to the thick substrate," *Electron. Lett.*, vol. 24, no. 17, pp. 1104–1106, 1988.
[11] I. Wolff and N. Knoppik, "Rectangular and circular microstrip disk capacitors and resonators," *IEEE Trans. Microwave Theory Tech.*, vol. MTT-22, pp. 857–864, Oct. 1974.
[12] W. C. Chew and J. A. Kong, "Effects of fringing field on the capacitance of circular microstrip disk," *IEEE Trans. Microwave Theory Tech.*, vol. MTT-28, pp. 98–104, Feb. 1980.
[13] L. C. Shen, S. A. Long, M. R. Allerding, and M. D. Walton, "Resonant frequency of a circular disc, printed-circuit antenna," *IEEE Trans. Antennas Propagat.*, vol. AP-25, pp. 595–596, July 1977.
[14] M. Abramowitz and I. A. Stegun, *Handbook of Mathematical Functions*. Nat. Bur. Stand. Appl. Math. Ser. 55, Washington, DC, June 1964.
[15] A. G. Derneryd, "Microstrip disc antenna covers multiple frequencies," *Microwave J.*, pp. 77–79, May 1978.
[16] ——, "Analysis of microstrip-disk antenna element," *IEEE Trans. Antennas Propagat.*, vol. AP-27, pp. 660–664, Sept. 1979.
[17] M. D. Deshpande and M. C. Bailey, "Input impedance of microstrip antennas," *IEEE Trans. Antennas Propagat.*, vol. AP-30, pp. 645–650, 1982.
[18] T. Itoh and R. Mittra, "Analysis of a microstrip disk resonator," *AEU*, vol. 27, no. 11, pp. 456–458, 1973.
[19] J. Q. Howell, "Microstrip antenna," *IEEE Trans. Antennas Propagat.*, vol. AP-23, pp. 90–93, Jan. 1975.

Target Discrimination Using Multiple-Frequency Amplitude Returns

MIN-CHIN LIN AND YEAN-WOEI KIANG

***Abstract*—A technique for radar target discrimination using multiple-frequency scattering amplitude data is investigated. Based on the concept of natural resonance frequencies, the technique proposed is aspect-angle independent. This is achieved through simple signal processing, thus providing a nearly real-time operation. The radar cross sections (RCS) of spheroids are calculated numerically to simulate the received radar returns for discriminating different spheroids and wires in the resonance frequency region. Simulation results also take into account the effect of noise which appears in practical measurement.**

Manuscript received April 27, 1989; revised January 10, 1990. This work was supported by the National Science Council, Republic of China, Grant NSC77-0404-E002-24.

The authors are with the Department of Electrical Engineering, National Taiwan University, Taipei, Taiwan, Republic of China.

IEEE Log Number 9038600.

I. Introduction

Research on system identification concerning obtaining information about a process from input-output data has been conducted for years. In electromagnetic scattering, characteristics of scatterers such as shape and size are to be found from the scattering data. However, it is quite difficult to fully identify the unknown target. Consequently, researchers have concentrated on the more tractable problem of deciding which of a set of possible targets is present, i.e., the discrimination problem.

It is well known that radar return in the resonance frequency region bears information about the crude shape of the scattering body [1]. Based on this, many investigations concerning discrimination of targets have been done in the resonance frequency band [2], [3]. However, most classification algorithms such as nearest neighbor (NN) rule [2], [3] use the amplitude returns (with or without phase) as the target features which are obviously aspect-dependent, and thus *a priori* information about the aspect angle is required. In practical situations, the aspect angle can be estimated [2] but is usually of low accuracy. If the operating frequency gets higher, the variations of radar returns with respect to aspect angle become more severe. Thus a little error in the estimation of aspect angle may bring serious difficulty to those discrimination methods.

The idea of aspect-independent natural frequencies established by the singularity expansion method (SEM), proposed by Baum [4] in the early 1970's, is another good starting point for target discrimination. The theoretical work of Marin [5] constructs the basic principle of SEM. According to SEM, the late-time scattering response from a variety of conducting scatterers can be represented as a series of damped sinusoids in time domain or as a series expansion of simple poles in frequency domain. Note that the damping corresponds to radiation loss. In a word, natural resonance frequencies are the effective characteristics of targets and are useful in the application to discrimination.

Indeed a lot of work has been done in either the frequency or time domain using the natural frequencies as target features. Since each target is characterized by a unique set of natural frequencies, a data base of known natural frequencies for the targets of interest, instead of the scattering data at many aspects, is prepared. In target discrimination, the natural frequencies of unknown targets are calculated from the received scattered field and an NN rule or other method is used as the decision criterion [6], [7]. However, usual methods for direct pole extraction are either time consuming [8] or seriously limited by noise [9]. To avoid these difficulties, convolving the scattering impulse response with the so-called "E-pulse," which is unique for each specific target to achieve the expected extinction performance is a technique developed in time domain [10], [11].

Instead of direct pole extraction, a frequency-domain discrimination scheme based on the concept of natural frequencies is proposed in this study. The method presented utilizes the fact that most targets of interest are high-Q structures thus having significant resonance phenomenon in radar cross section (RCS). Generally speaking, targets of long and thin shape are considered to have higher Q value in comparison with spheres by their distribution of natural reso-